

Isolated Three-Phase Rectifier Unit with High Power Factor

Elias Sebastião de Andrade, Denizar Cruz Martins and Ivo Barbi
Dept. of Electrical Engineering - Power Electronics Institute
Federal University of Santa Catarina
P.O. BOX: 5119-88040-970 - Florianópolis-SC-BRAZIL
Tel.: (55) 482.31-9204 - FAX: (55) 482 31-9770
E.MAIL: inep@inep.ufsc.br

Abstract - This paper presents the analysis of an isolated three-phase converter operating in soft-commutation as a battery charger. The structure works with high power factor without intermediate circuits. Its main features are: simplicity of control driver circuit and robustness of power circuits. Principle of operation, design procedure, simulation and experimental results obtained from a laboratory prototype (55A/48V) are presented.

I. INTRODUCTION

Recently the research in the three-phase power converters area with high power factor has been intensified, e.g. [6] [7] [8]. Some factors must also be present, such as the conversion of the input alternating voltage to regulated output continuous voltage, isolated output, soft commutations and a lower number of controlled switches.

The topology of the converter presented here is particularly simple and permits the design of a robust piece of equipment at lower cost, for the following reasons: it does not need low frequency filters either in the input or in the output; the losses during the commutation are practically null; the drive circuit is very simple.

With this topology, we can obtain the fundamental characteristics for the desired application, that is, galvanic isolation between the source and the converter, simple drive control, possibility of control of power flux through frequency modulation of two switches per phase, intrinsic output characteristic such as current source, besides a small output current ripple. It has another important characteristic, that is, a high power factor without the need for intermediate correction circuits.

II. PROPOSED CIRCUIT

2.1 Circuit Description

This converter has in the input a full-wave rectifier followed by a series-resonant circuit with voltage clamping in the resonant capacitor.

The proposed resonant converter diagram is shown in Fig.1, with:

v_{ac} → input AC voltages;
 E_o → battery voltage;
 D1-D12 → input rectifier diodes;
 DP1-DP6 → output rectifier diodes;
 DG1-DG6 → voltage clamping diodes;
 T1-T6 → controlled switches;
 Lr1-Lr3, Cr1-Cr6 → resonant inductors and capacitors.

The T1, T3 and T5 switches are driven simultaneously, the same for T2, T4 and T6. For this reason the drive circuit becomes very simple.

In the laboratory prototype that was built we put resistors in parallel with E_o to absorb all power.

2.2 Operation Principle

The operation of this converter is based on some basic principles, such as: (1) the switching frequency is much greater than the input source frequency; (2) the battery voltage, E_o , is much lower than the input source peak voltage V_m , so that θ_1 (initiation angle) is very small; and (3) the inverter stage in steady state works with constant frequency.

For a quarter of period of the input source voltage there are two different modes of operation, as is shown in Fig.2.

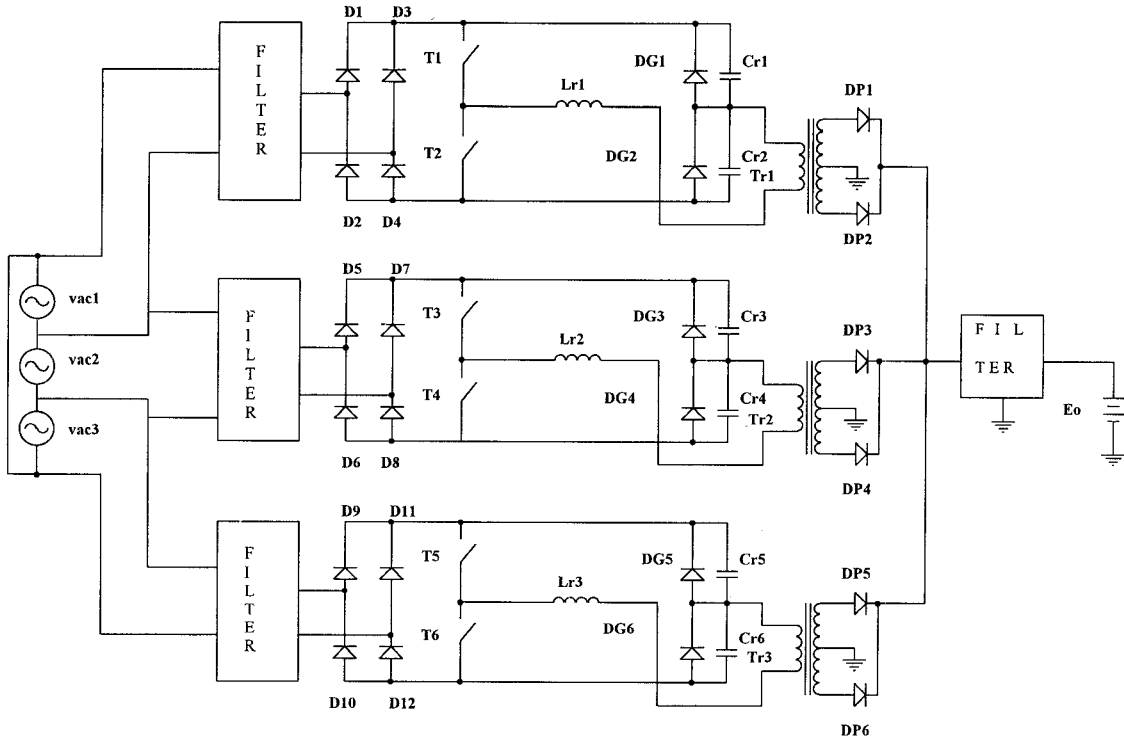


Fig.1: Proposed circuit diagram.

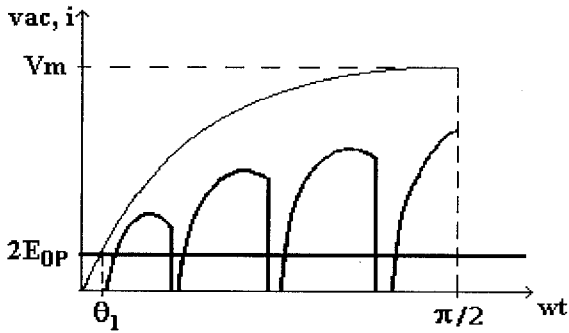


Fig.2: Input source voltage and current.

Mode A: $(0 < \theta_1 < \pi/2) \rightarrow v_{ac} < 2 \cdot E_{OP}$. There is no power transfer to the load.

Mode B: $(\theta_1 < \theta < \pi/2) \rightarrow$ During this interval, the converter delivers energy to the load.

So:

$$\sin \theta_1 = \left(\frac{2 \cdot E_{OP}}{V_m} \right) \Rightarrow \theta_1 = \arcsin(q) \quad (1)$$

$$\cos \theta_1 = \sqrt{1 - \sin^2 \theta} = \sqrt{1 - q^2} \quad (2)$$

The parameter “q” is the voltage static gain and E_{OP} is the secondary voltage of the transformer reflected to the primary.

2.3. Operation Stages

During a switching cycle of the resonant converter, the input voltage v_{ac} can be considered constant. Therefore, the structure to be analyzed is shown in Fig.3, where the voltages V_{in} and E_o are considered constant and all the components are considered ideal.

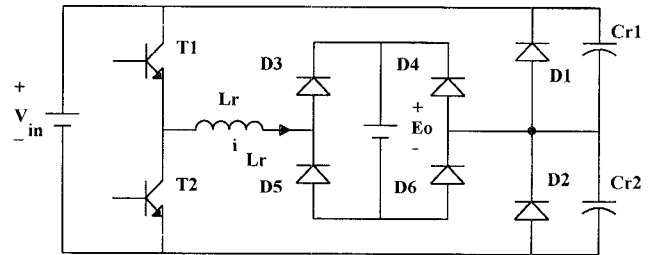


Fig.3: Analyzed structure.

First Stage (t_0, t_1 -resonant)-T1, D3, D6 are conducting:

Initial conditions: $i_{Lr}=0; v_{Cr1}=V_{in}; v_{Cr2}=0$.

The transistor T1 is conducting and i_{Lr}, v_{Cr1} and v_{Cr2} evolve sinusoidally. When $v_{Cr2}=V_{in}$ the diode D1 is forward biased.

Second Stage (t_1, t_2 -linear) - T1, D3, D6, D1 are conducting:

Initial conditions: $i_{Lr}=1$; $v_{Cr2}=V_{in}$; $v_{Cr1}=0$.

The diode D1 starts to conduct, the current i_{Lr} decreases linearly down to 0, the voltages v_{Cr1} e v_{Cr2} maintains the same values.

Third Stage (t_3, t_4 -resonant)-T2, D4, D5 are conducting :

Initial conditions: $i_{Lr}=0$; $v_{Cr1}=0$; $v_{Cr2}=V_{in}$.

In this stage the same operation mode of the first stage is repeated.

Fourth Stage (t_4, t_5 -linear)-T2, D4, D5, D2 are conducting:

Initial conditions: $i_{Lr}=-1$; $v_{Cr1}=0$; $v_{Cr2}=V_{in}$.

The same operation mode of Second Stage is repeated here.

Final conditions:

$$i_{Lr}=0 - v_{Cr1}=V_{in} - v_{Cr2}=0.$$

The turn off of the transistors T1 and T2 occurs naturally, characterizing a zero current switching (ZCS).

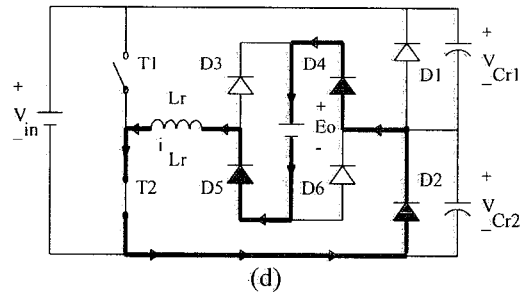


Fig.4: (a,b,c,d) - Operation Stages.

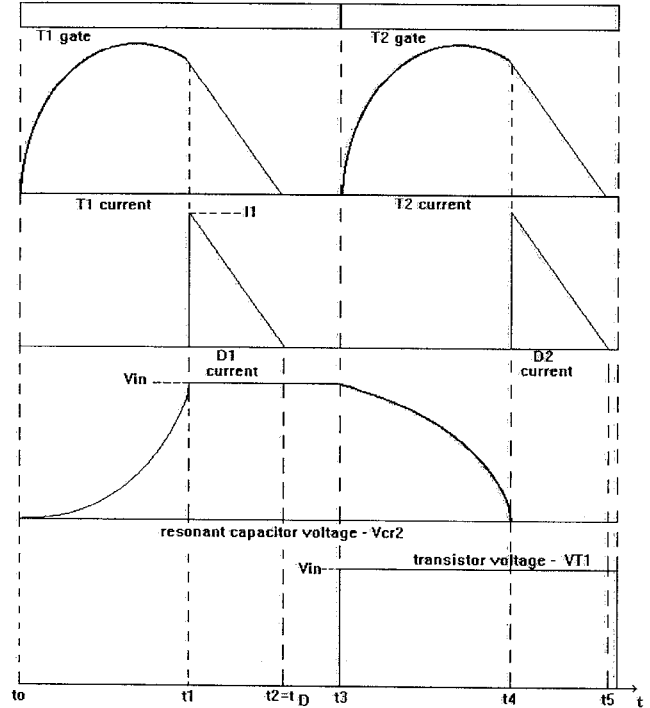
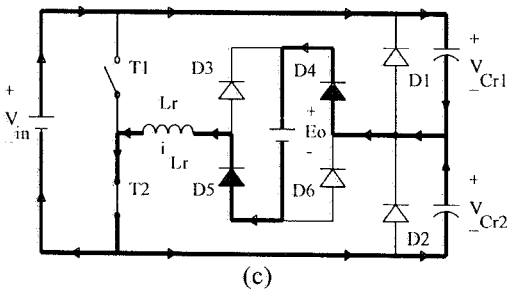
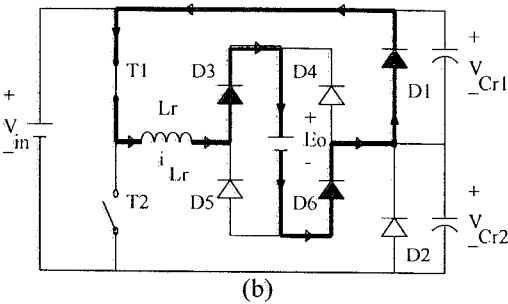
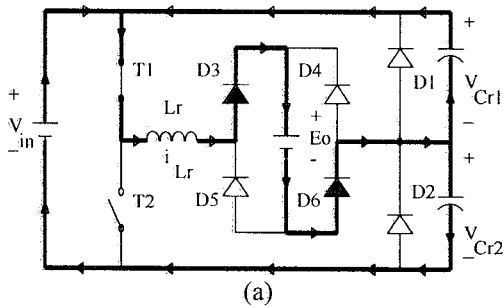


Fig.5: Main waveforms.

III. MATHEMATICAL ANALYSIS

Through mathematical analysis, we can determine the stress through the components of the prototype, as well as its power transfer characteristics. In this study we have presented the essential curves to make the simulation of the converter possible.

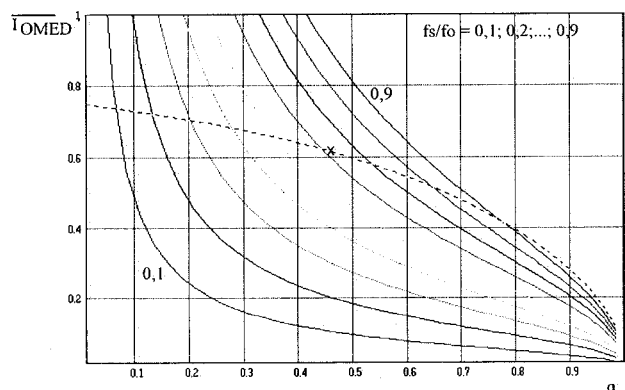
3.1 -Relevant Curves and Expressions

Equation (3) proves that the output current is a function of the operation frequency and the voltage static gain. Figure 6a presents the characteristic curves relating different switch commutation frequencies to static gain.

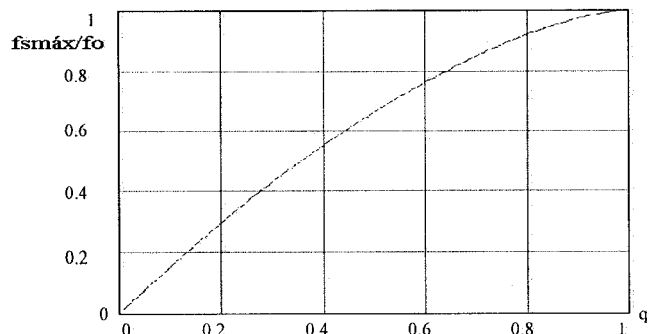
$$\overline{I_{OMED}} = \frac{3 \cdot V_m \cdot f_s}{4 \cdot \pi^2 \cdot f_o \cdot E_{OP}} \left(\pi - 2 \text{sen}^{-1} q + 2 \cdot q \cdot \sqrt{1 - q^2} \right) \quad (3)$$

$$\overline{I_{OMED}} = \frac{Z_o}{V_m} \cdot \left(I_{OMED} \cdot \frac{N_s}{N_p} \right) \quad (4)$$

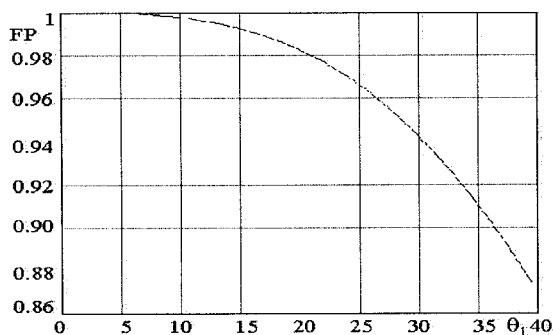
Other curves, such as: behavior of current and voltage on switches, diodes, capacitors and inductors are shown in [2] with their respective deductions.



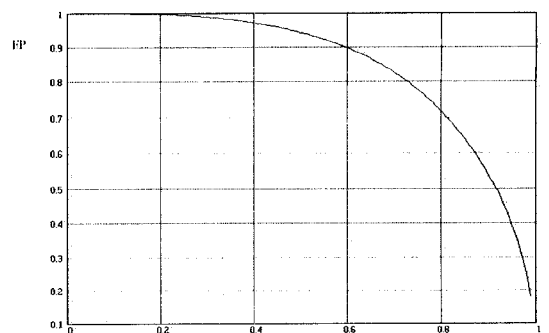
(a) Output characteristic.



(b) Relation between fsmax/fo and q.



(c) Relation between PF and θ_1 .



(d) Relation between PF and q.

Fig.6 (a,b,c,d) - Design Curves.

The dashed line, Fig.6a, represents the limit where the conduction becomes continuous. Operation points above it, denote the loss of “ZCS” characteristic.

Relating (2) to (5), (6) is obtained. It is observed that the PF of the structure is an exclusive function of the static voltage gain.

$$PF = 1 - \frac{2 \cdot \theta_1 - 2 \cdot \text{sen}(2 \cdot \theta_1)}{\pi} \quad (5)$$

$$PF = 1 - \frac{2 \cdot \text{sen}^{-1} q - 2 \cdot q \cdot \sqrt{1 - q^2}}{\pi} \quad (6)$$

With the same relations between frequencies for a lower value of “q” we can obtain a greater power factor in the structure, but this implies an increase in the currents that cross the elements of the circuit, which influences the yield, through the increase in conduction loss and in the specification in the current of the components. There is a relation between PF and “q” which can be optimized according to the characteristics required.

Especially in the case of a variable entrance, the operation should be in discontinuous conduction, even in maximum input voltage (greater energy stored in the resonant inductor). Thus, the relation between the frequency of operation and the resonance is calculated, in order to guarantee that the power transistor commutation takes place with zero current ($V_{in}=V_m$).

In the commutation cycle, there are two resonant stages and two free-wheel stages. For Fig. 5 (disregarding dead time and command pulses), the following equation is obtained:

$$T_s = \frac{1}{f_s} = 2 t_1 + 2 t_D = 2 (t_1 + t_D) \quad (7)$$

Remembering that:

$$T_0 = \frac{1}{f_0} = \frac{2 \cdot \pi}{\omega_0} \quad (8)$$

The following expression can be obtained, relating the frequencies to static gain.

$$\frac{f_{s\max}}{f_o} = \frac{\pi}{\cos^{-1}\left(\frac{q}{q-2}\right) + \frac{2}{q}\sqrt{1-q}} \quad (9)$$

Equations for dimensioning semi-conductors, whose mathematical deductions are in [4], are presented below.

- Mean current in the clamping diodes:

$$\overline{i_{DG\text{MED}}} = \frac{f_s}{4 \cdot \pi^2 \cdot f_o \cdot q} \cdot (\pi - 2 \cdot \text{sen}^{-1}q - 2 \cdot q \cdot \sqrt{1-q^2}) \quad (10)$$

- Mean current in the power switches:

$$\overline{i_{T\text{MED}}} = \frac{f_s}{4 \cdot \pi^2 \cdot f_o \cdot q} \cdot (\pi - 2 \cdot \text{sen}^{-1}q + 2 \cdot q \cdot \sqrt{1-q^2}) \quad (11)$$

- Effective current in the clamping diodes:

$$\overline{i_{DG\text{EF}}}^2 = \frac{4 \cdot f_s}{f_o \cdot 3 \cdot \pi^3 \cdot q} \cdot (1-q^2) \cdot (1-q)^{3/2} \quad (12)$$

- Effective current in the power switches:

$$\overline{i_{T\text{EF}}}^2 = \frac{f_s(1-q^2)}{2\pi^3 f_o} \left[(2-q)^2 \cos^{-1}\frac{q}{q-2} + 2q\sqrt{1-q} + \frac{8}{3q}(1-q)^{3/2} \right] \quad (13)$$

- Peak current in the clamping diodes:

$$\overline{i_{DGp}} = \sqrt{(1-q)} \quad (14)$$

- Peak current in the power switches:

$$\overline{i_{Tp}} = \left(\frac{2-q}{2} \right) \quad (15)$$

- Effective current in the resonant inductor:

$$i_{Lr} = \sqrt{i_{T1\text{EF}}^2 + i_{T2\text{EF}}^2} = \sqrt{2} \cdot i_{T\text{EF}} \quad (16)$$

The current in the output rectifier diodes is the same as that which flows through the power transistor, multiplied by the transformation relation (N_p/N_s). Therefore, the expressions (11), (13) and (15) are valid for dimensioning these rectifiers.

3.2 Design procedure and example

According to the required characteristics, input and output, after choosing the switch technology, it is possible to design and simulate the battery charger. We can summarize in 5 steps the converter open-loop design (with

“q” fixed). In this case, the converter is designed to charge four batteries connected in series.

$I_{\text{OMED}}=55.0$ A (average output current)
 $V_{\text{rms}}=380$ V (rms input voltage)
 $f_{s\max}=30.0$ kHz (maximum switching frequency)
 $\text{PF}_{\min}=0.95$ (minimum power factor)
 $E_0=48.0$ V (output voltage)

1st. step: From PF_{\min} and Fig.6.c or (5) we obtain the initial angle θ_1 , that is the initial power transfer angle ($\theta_1=0.5$ rad = 28.5°);

2nd. step: From PF_{\min} we determine “q” through (6) - $q = 0.48$;

3rd. step: With “q” it is possible to determine voltage of the primary side of the transformer and the its relation with the secondary ($N_p/N_s=E_{op}/E_o$), ($E_{op}=128.4 - N_p/N_s=2.7$);

4th. step: From Fig.6.b or (9) we obtain the resonant frequency f_o ($f_o \cong 47$ kHz);

5th. step: From f_o , f_s , PF_{\min} , “q” and the following equations, we can obtain the resonant parameters:

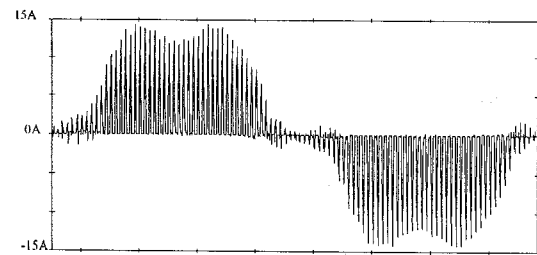
$$I_{\text{OMED}} = \frac{3 \cdot f_s \cdot \text{FP}_{\min}}{2 \cdot \pi \cdot q \cdot f_o \cdot \eta} \cdot \frac{V_m}{\sqrt{L_r/C_r}} \cdot \frac{N_p}{N_s} \quad (17)$$

$$f_o = \frac{1}{2 \cdot \pi \cdot \sqrt{L_r \cdot C_r}} \quad (18)$$

For η (efficiency) = 0.88:
 $Z_o = 13.96\Omega$; $L_r = 47.3\mu\text{H}$; $C_r = C_{r1} + C_{r2} = 243\eta\text{F}$.

IV. SIMULATION AND EXPERIMENTAL RESULTS

Fig.7 shows the main waveforms obtained by simulation, which present the following results: $P_0=2.8$ kW; $\text{PF}=0.98$ and $\theta_1=0.52$ rad.



(a) Input Current

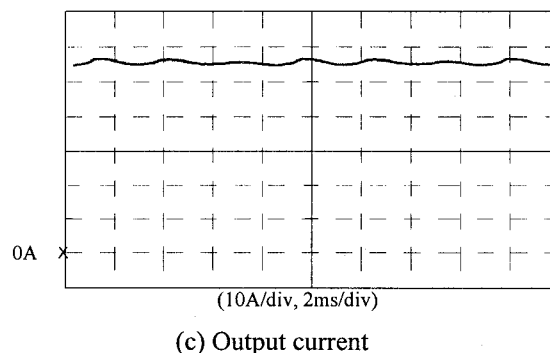
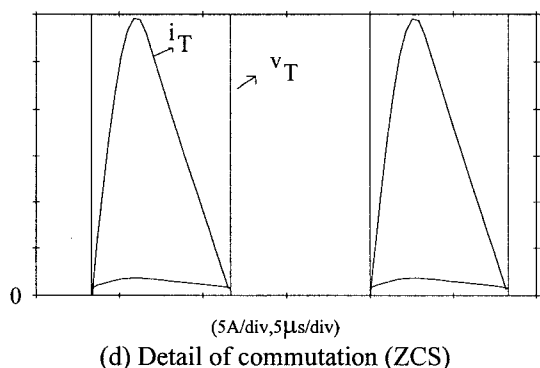
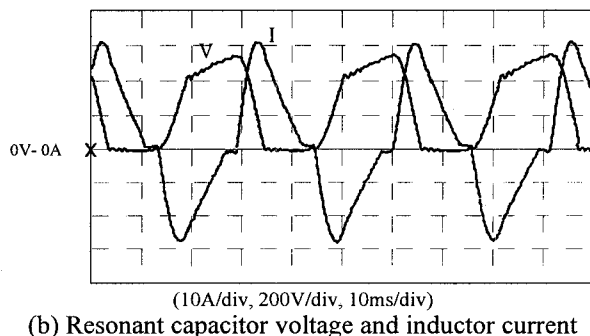
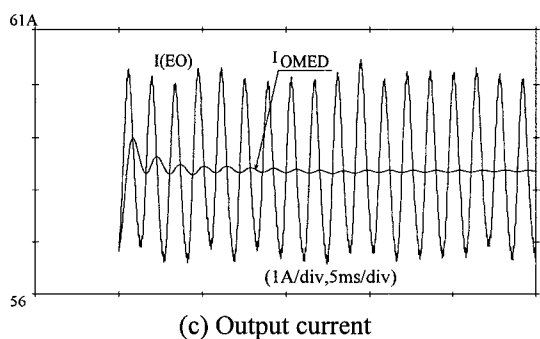
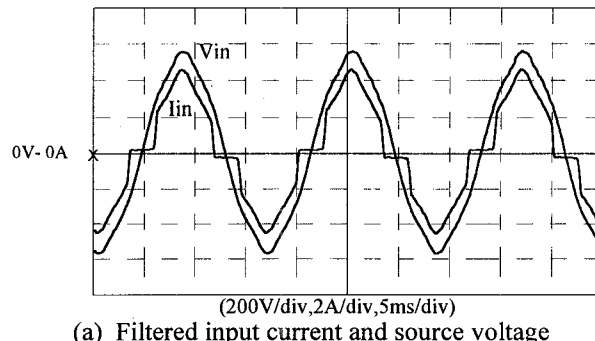
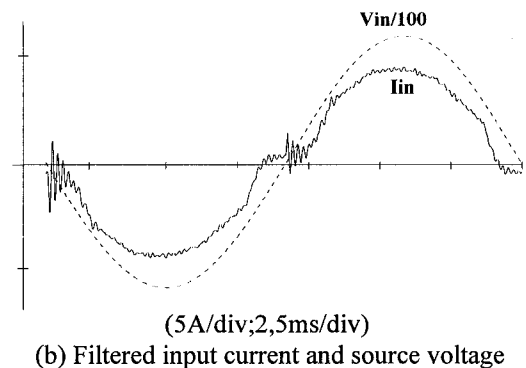


Fig.7: (a,b,c,d) Simulation results.

Fig.8: (a,b,c) Experimental results

In Fig.8a we have the line input voltage and filtered input current. As we can observe, the source voltage available in the lab has harmonic distortion, and the current follows its form. In Table 1 we have the measured values obtained from the prototype.

The 360 Hz ripple appears because the output current is a sum of three currents displaced of 120 degrees.

In Fig.9 we can see the efficiency curve built with points (efficiency $\times f_s$) for constant "q". The most relevant losses come from output rectifiers and magnetics, which can be improved.

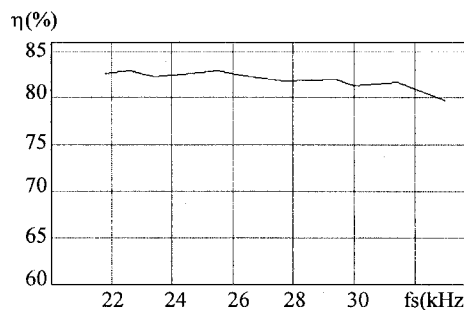


Fig.9 - Efficiency curve

Table 1 - Measured values for nominal conditions

phase	TDH I(%)	TDH V(%)	FP
R	23,6	3,4	0,973
S	22,35	3,4	0,976
T	20,76	3,3	0,980

V. CONCLUSION

The converter we have studied behaves according to the mathematical analysis previously developed. It presents a high power factor without intermediate circuits, a lower number of active switches and simple control. The circuit driver generates complementary pulses that turn on each one of the switches of the each phase, instantaneously and in isolation.

The operation frequency determines the output power. The efficiency can be improved by use of the better semiconductors (mainly diodes) and careful study of magnetics.

Its current source characteristic easily offers the possibility of parallel association. The three-phase input diminishes drastically the ripple of the output current.

VI. REFERENCES

- [1] - I. Barbi and E. Kassick. "A Low Cost High Power Factor Resonant Mode Battery Charger". In: APPLIED POWER ELECTRONICS CONFERENCE, 1993. APEC'93: Conference record, p.543-8.
- [2] - E. Andrade. "Carregador de Baterias Série Ressonante, Isolado, com Grampeamento da Tensão sobre o Capacitor Ressonante, Alimentação Trifásica e Alto Fator de Potência". Dissertation Master Thesis, INEP, UFSC - Brazil, 1994.
- [3] - E. Andrade. "Isolated Three-Phase Resonant Converter with High Power Factor". In: 3rd BRAZILIAN POWER ELECTRONICS CONFERENCE, 1995. COBEP'95: Conference record, p.353-8.
- [4] - J. Ferreira Neto. "Estudo e Implementação de um Sistema Carregador de Baterias Operando no Modo Ressonante com alto fator de Potência Utilizando IGBT's". Dissertation Master Thesis, LAMEP, UFSC - Brazil, 1994.
- [5] - G. Ferret. "Estudo de uma Fonte Ressonante com Entrada Trifásica e Alto Fator de Potência Saída Isolada". Dissertation Master Thesis, LAMEP, UFSC - Brazil, 1994.
- [6] - T. Latos and D. Basack. "A High Efficiency 3 kW Switchmode Battery Charger". In: IEEE POWER ELECTRONICS SPECIALISTS CONFERENCE, 1982. PESC'82: Conference record, p.341-9.
- [7] - D. Simonetti, J. Sebastian and J. Uceda. "Single-Switch Three Phase Power Pre-Regulator under Variable Switching Frequency and Discontinuous Input Current". In: IEEE POWER ELECTRONICS SPECIALISTS CONFERENCE, 1993. PESC'93, : Conference record, p.657-61.
- [8] - P. Ziogas, S. Manias and A. Prasad. "An Active Power Factor Correction Technique for Three Phase Diode Rectifiers". In: IEEE POWER ELECTRONICS SPECIALISTS CONFERENCE, 1989. PESC'89 : Conference record p. 58-65.